Research Article

Meltem Coşkun, Ecem Özen Öner, Cengiz Tatar and Mediha Kök*

MgO NPs reinforced PCL/PVC nanocomposite films with enhanced UV shielding and thermal stability for packaging applications

https://doi.org/10.1515/phys-2025-0240
Received June 23, 2025; accepted October 26, 2025;
published online December 3, 2025

Abstract: In this study, poly(ε-caprolactone) (PCL) and polyvinyl chloride (PVC) nanocomposite films reinforced with magnesium oxide (MgO) nanoparticles were successfully fabricated for potential use in UV-shielding packaging and optoelectronic applications. Composites containing 10, 20, and 30 wt% MgO were prepared via the solution casting method, and their structural, morphological, thermal, and optical characteristics were comprehensively analyzed using FTIR, XRD, SEM, DSC, TGA, and UV–Vis spectroscopy. FTIR and XRD results confirmed strong interfacial interactions between MgO nanoparticles and polymer chains, accompanied by a notable enhancement in crystallinity with increasing MgO content. SEM micrographs revealed uniform dispersion with limited agglomeration observed at 30 wt% MgO, supporting the morphological consistency of the composites. DSC and TGA analyses demonstrated that MgO acts as a nucleating and thermally stabilizing agent, leading to improved crystallization behavior and higher residual mass. Optical investigations indicated that MgO incorporation enhanced UV absorption capability and reduced the optical band gap from 5.77 eV (pure blend) to 4.88 eV (30 wt% MgO), confirming improved photon–matrix interaction. In addition, the films exhibited a reversible shape memory effect, allowing recovery of their original form after thermal stimulus. Considering their low density, environmental compatibility, and cost-efficient fabrication, MgO-reinforced PCL–PVC nanocomposites are proposed as promising, scalable, and economically viable materials for advanced packaging, biomedical, and flexible optoelectronic applications.

***Corresponding author: Mediha Kök**, Department of Physics, Faculty of Science, Firat University, Elazığ, Turkey, E-mail: msoglu@firat.edu.tr
Meltem Coşkun, **Ecem Özen Öner and Cengiz Tatar**, Department of Physics, Faculty of Science, Firat University, Elazığ, Turkey.
https://orcid.org/0000-0002-0876-9071 (C. Tatar)

Keywords: PCL; PVC; MgO nanoparticles; nanocomposite; optical properties; thermal stability

1 Introduction

Currently, the protection of sensitive products such as fresh food, pharmaceuticals and electronic devices from spoilage is only possible with effective packaging systems. Due to inadequate packaging, food waste reaches serious levels, the effectiveness of pharmaceuticals decreases and electronic devices can be damaged. In this context, polymer-based packaging materials are replacing traditional materials with their advantages such as lightness, low cost, flexibility, and barrier properties against oxygen and moisture. In particular, innovative materials developed through polymer nanotechnology offer great contributions in terms of food safety, shelf life and environmental sustainability. Today, polymers used in the packaging industry constitute a significant portion of the global market, creating both economic and technological value [1–5].

Polycaprolactone (PCL) is a biodegradable polyester of synthetic origin and an important biopolymer widely used in the biomedical and packaging industries. It offers advantages in different fields thanks to its hydrophobic structure, low melting point (59–64 °C), high formability and resistance to various solvents. Enzymatically degradable in the biological environment, PCL is safely used in drug delivery systems, surgical sutures, tissue engineering scaffolds and medical implants. Although its biocompatibility is limited, its flexibility and blendability make it a versatile material. It is also used in some FDA-approved medical products. PCL, which is also used in food packaging, is of great importance in terms of environmental sustainability thanks to its controlled degradability and offers an alternative to traditional plastics in this respect [6–10].PVC (polyvinyl chloride), with its rigid to very flexible structure, is used in a wide range of products from short-lived packaging to long-lasting building materials. It is widely used in applications such as pipes,

window profiles and cable coverings in the construction industry, as well as flooring, wall coverings, toys, clothing, packaging and advertising products. The main reason why PVC can be used in so many areas is the polarity of the carbon-chlorine bond in its structure, which enables it to interact strongly with additives. This structure allows the properties of the material to be changed as desired with additives. In addition to its low cost, PVC's advantages such as high chemical resistance, good mechanical properties, weather and water resistance make it indispensable in industry. It also has many additional properties such as transparency, impact resistance, formability and flexibility. PVC has been in production since the 1930s and today ranks third in the world in terms of production volume [11–14].

Polymer blends are a research topic that attracts attention both in industry and academia. Systems formed by blending different polymers can be either single-phase homogeneous or multiphase heterogeneous; multiphase structures are more common, usually due to thermodynamic incompatibility. PCL and PVC are one of the rare polymer pairs that are compatible in the amorphous phase at all composition ratios. In this system, the crystalline phase consists only of pure PCL; as the PVC content increases, the melting temperature of PCL decreases and the amorphous regions expand, but the crystalline structure does not change. Furthermore, spherulite formation is observed in this blend, but the spherulite growth rate of PCL slows down when non-crystallizable PVC is added [15, 16].

Recent developments in polymer nanocomposites obtained by adding different nanomaterials have shown significant improvements in the structural, optical, and functional properties of polymer matrices. For example, it has been demonstrated that adding SiN_4/TaC nanoparticles to polymer composites improves structural stability and electrical conductivity, paving the way for potential electronic applications [17]. Likewise, hybrid nanoparticles, such SiO_2/Cr_2O_3, have enhanced morphological, optical, and antibacterial qualities in biopolymer blends, increasing their applicability in optical nanodevices and food packaging [18]. The functional range of polymer-based materials in sensor and quantum electronic applications is further expanded by the reported significant enhancement of dielectric, optical, and pressure sensing properties through the incorporation of metal oxide nanoparticles such as MnO_2 and $BaTiO_3$ within polymer matrices [19, 20]. These developments highlight how crucial it is to include nanoparticles into polymer composites in order to customize them for multipurpose packaging solutions that satisfy contemporary requirements for environmental sustainability, durability, and food safety. One popular technique for enhancing UV protection in packaging is the addition of metal oxide nanoparticles to polymer matrices [21]. Due to their strong UV absorption capability, ZnO, TiO_2, and SiO_2 nanoparticles are commonly chosen. Nonetheless, the performance of composites is strongly impacted by the uniform dispersion of nanoparticles within the polymer. MgO nanoparticles have drawn attention recently as a substitute filler for thermal stability and UV protection [21, 22]. Nanomaterials, especially nanofibers and metal oxide nanoparticles such as magnesium oxide (MgO), are valuable for both research and industry due to their unique properties. MgO is characterized by its thermal stability, biocompatibility, low toxicity and antibacterial effects. When doped with polymers, MgO improves mechanical strength, thermal resistance and barrier properties, making these composites ideal for medical, packaging, sensor, membrane and energy storage applications. When combined with biodegradable polymers, MgO-based composites also support sustainable and environmentally friendly solutions [23–27]. MgO-reinforced polymer composite films can potentially be useful for various applications due to MgO's antibacterial properties. Additionally, they can be used as scaffolds in tissue engineering, bandages, and wound dressings in the biomedical field; they can also be used for controlled release in drug delivery systems. In the environmental field, they can be tested in water purification membranes and UV protective coatings, and in the food industry, they can be used as antimicrobial packaging materials to extend the shelf life of foods. Finally, they facilitate the use of electronic and sensor technologies, including dielectric layers and gas sensors [28–31].

This study, unlike previous studies, investigates the effect of MgO nanoparticles on the structural, thermal, and optical properties of PCL–PVC nanocomposites, particularly for UV-protective packaging applications. PCL–PVC-based nanocomposite films reinforced with MgO nanoparticles were synthesized. The structural, thermal, and optical properties of the obtained composites were investigated using detailed characterization techniques.

2 Experimental

2.1 Production of MgO nanoparticles and polymer composites

2.1.1 Step: MgO nanoparticle

The hydrothermal method was preferred to produce magnesium oxide nanoparticles. The hydrothermal method

stands out as a widely preferred and effective technique for nanomaterial synthesis. This process produces products with uniform shape and good crystallinity by allowing controlled crystal formation at high temperatures and pressures.

Additionally, using water as a solvent provides a nontoxic and more environmentally friendly method. Economic benefits of hydrothermally produced materials typically include minimal energy use and very simple equipment. However, the method's drawbacks include the demand for specialist equipment because to its high pressure requirements and lengthy reaction times. Furthermore, undesired phases may occur and product purity may decline if process parameters are not carefully regulated. For these reasons, the hydrothermal method's suitability should be carefully assessed in light of the material's characteristics and the synthesis goals [32–34].

Magnesium nitrate hexahydrate [$Mg(NO_3)_2{\cdot}6H_2O$, 99 % purity, Sigma-Aldrich] was needed as a precursor to produce magnesium oxide. Deionized water was preferred as the solvent in the synthesis processes. All chemicals were of analytical purity and were used without any purification process. 0.5 M $Mg(NO_3)_2{\cdot}6H_2O$ was dissolved in deionized water with a suitable magnetic stirrer to obtain a homogeneous solution. Additionally, NaOH solution was prepared in a separate place to adjust the pH of the process. The solution was made basic (pH: 10) with the help of a pH meter. During production by hydrothermal method, the pH value of the solution is of critical importance depending on the type of material to be synthesized, the desired phase, morphology and crystal structure. The resulting solution was transferred to a teflon-lined autoclave after pH adjustment and hydrothermal treatment was applied at constant temperature (180 °C for 12 h). After the hydrothermal treatment, the system was left to cool to room temperature, the precipitate was centrifuged and washed several times with deionized water and ethanol. The solid product obtained was dried in an oven (4 h at 50 °C). The dried product was then baked at 600 °C for 2 h to ensure the formation of the MgO crystal structure. The aim here is to calcinate the product obtained by hydrothermal means.

2.1.2 Step: nanocomposite thin film

In order to produce polymer blend films, the blend was first prepared using 0.3 g poly(ε-caprolactone) (PCL) and 0.2 g polyvinyl chloride (PVC). The MgO (magnesium oxide) compound was then dissolved in THF (tetrahydrofuran) solvent for 1 h and 54 min using a homogenizer device and then placed on a magnetic stirrer. 0.3 g of PCL polymer was first added to the blend and the temperature of the device was set to approximately 80 °C and PCL was completely dissolved. After PCL dissolution, 0.2 g of PVC polymer was added to the solution and the mixture was stirred until a homogeneous structure was obtained. The homogeneous mixture was spread uniformly on the surface using a film applicator device and composite materials in thin film form were obtained. This process was repeated for three different batches with MgO additives of 10 %, 20 % and 30 % (Table 1). Image of produced blend and MgO-blend nanocomposite were given in Figure 1.

Table 1: Mass rate of blend and nanocomposite components.

		PCL	PVC	Quantity MgO
Composite	Blend	0.3	0.2	–
	10 % MgO	0.3	0.2	0.05(g)
	20 % MgO	0.3	0.2	0.1(g)
	30 % MgO	0.3	0.2	0.15(g)

2.2 Characterization techniques of nanocomposites

In this study, various characterization techniques were used to determine the structural, morphological, thermal and optical properties of PCL–PVC blend and MgO doped composite films. Firstly, fourier transform infrared spectroscopy (FTIR) analysis was performed to determine the chemical functional groups. These measurements were taken in the wavenumber range of 500–4,500 cm^{-1} to investigate the

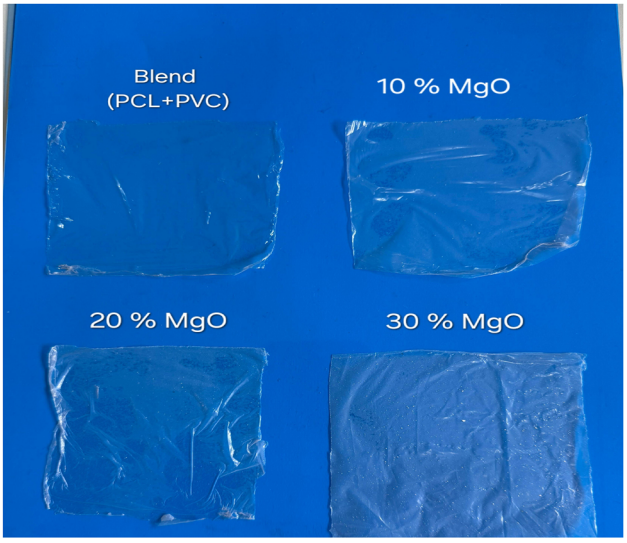

Figure 1: Images of blend film and their MgO composites.

interactions and possible bond changes in the film matrix. X-ray diffraction (XRD) analysis was performed to determine the crystal structure of the composites. XRD measurements were performed with an X-ray diffractometer operating in the range of $2\theta = 20–80°$ at room temperature. This investigation assessed the impact of MgO doping on the crystal structure as well as the existence of crystalline or amorphous phases. Scanning electron microscopy (SEM) was used to examine the distribution of particles and their surface appearance. SEM images were utilized to examine the distribution of MgO nanoparticles inside the film matrix, assess surface smoothness, and identify potential agglomerations. Differential Scanning Calorimetry (DSC) analysis was performed to determine the phase transition temperatures. DSC measurements were performed in the temperature range of 20–250 °C and parameters such as melting temperature (T_m) and glass transition temperature (T_g) were evaluated. Thermo gravimetric analysis (TGA) was applied to evaluate the thermal stability of the composites. TGA analyses were performed in the range of 20–500 °C and decomposition temperatures and mass losses were analyzed. Finally, the optical properties of the film samples were evaluated using UV-Visible Region Spectroscopy (UV–Vis). Measurements were taken in the wavelength range of 200–900 nm and light transmittance, opacity values and band gap were calculated by Tauc method.

3 Results and discussions

The FTIR spectra of pure PCL–PVC polymer blend and nanocomposites containing 10 %, 20 % and 30 % MgO are presented comparatively in Figure 2. FTIR analysis can be used to identify functional groups in the composite structure and to determine the level of interaction between MgO and the polymer matrix. In the pure PCL–PVC blend spectrum, the strong absorption band at approximately 1,720 cm^{-1} corresponds to the stretching vibration of the ester carbonyl group of the polycaprolactone (PCL) component [35, 36]. In addition, the 2,940 cm^{-1} and 2,860 cm^{-1} bands indicate aliphatic C–H stretching, while the 1,240–1,040 cm^{-1} band indicates C–O–C stretching vibrations [37]. With the further incorporation of MgO nanoparticles into the composite structure, new absorption bands in the range of 600 to 400 cm^{-1} appeared. These bands, which correspond to the vibrational modes of Mg–O bonds, have been identified as specific to this in previous research [38, 39]. These bands became more pronounced, especially in the composite containing 30 % MgO. This result indicates that the additive was more densely packed and efficiently dispersed in the polymer matrix. A significant decrease in the intensity of the carbonyl band around 1,720 cm^{-1} was also observed as the MgO content increased. This implies that MgO particles form physical or chemical bonds through hydrogen bonds or surface interactions. Similarly, the bandwidth and intensity changed in the region of C–O–C stretching vibrations. Such changes imply that the filler can alter the molecular order in the matrix and create new interactions between polymer chains [40]. As a result, hydrogen bonding and surface adsorption effects are the main ways that MgO nanoparticles and the PCL-PVC matrix interact. New interchain contacts are produced when the hydroxyl groups on the MgO surface form bonds with the carbonyl (C=O) and C–O–C groups of PCL. By changing the matrix's molecular configuration, this method improves the composite's mechanical, thermal, and barrier qualities [41]. Such research also shows that the composite can be improved through such interactions.

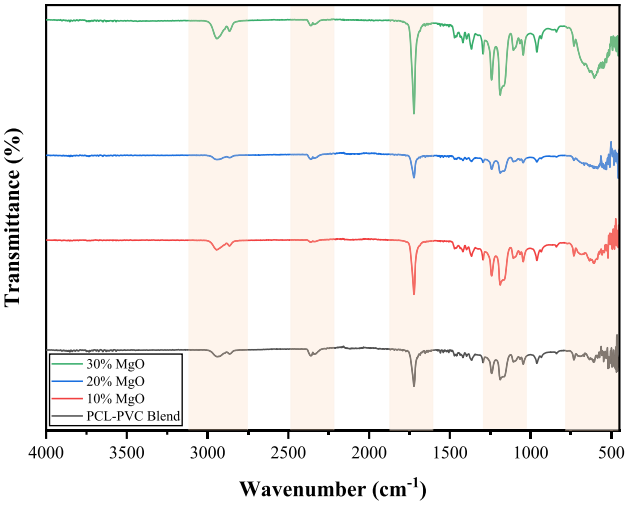

Figure 2: FTIR spectra of PCL–PVC blend and their composites.

The graph displays the X-ray diffraction (XRD) (Crystal structure and phase analysis) patterns of the mix that includes composites with 10 %, 20 %, and 30 % MgO additions to the polymer matrix (PCL + PVC) (Figure 3). Additionally, provided as a reference is the XRD pattern of pure MgO. The distinctive diffraction peaks of MgO's cubic crystal structure may be seen in the pure MgO pattern. In accordance with JCPDS card number 01-071-1,176 [42, 43], these peaks: $2\theta \approx 36.9°$ (200), $2\theta \approx 42.9°$ (220), $2\theta \approx 62.3°$ (222), $2\theta \approx 74.7°$ (400), and $2\theta \approx 78.6°$ (420) confirm the crystalline structure of MgO. The blend sample does not show any clear, sharp peaks [44]. This suggests that there are no regular long range crystalline areas and that the amorphous structure is predominant. In general, PCL and PVC can both have amorphous or semi crystalline characteristics

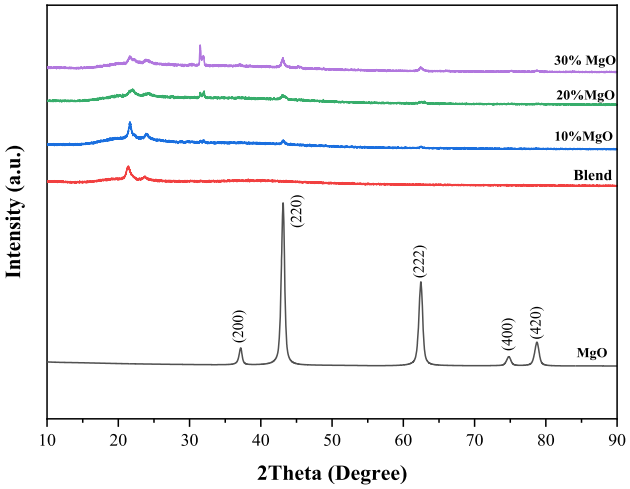

Figure 3: X-ray diffractograms of MgO nanoparticles (NPs), PCL-PVC blend and their nanocomposites.

[44–46]; however, when combined, this crystallinity can be further diminished. The peaks that resemble the pure MgO pattern become more noticeable in composites that contain 10 %, 20 %, and 30 % MgO, according to the patterns of MgO doped composites. The existence of MgO is confirmed by the peaks located at 36.9°, 42.9°, and 62.3° in particular. The crystalline structure of MgO in the composite is maintained and distributed, as evidenced by the fact that the intensity of these peaks rises with increasing MgO content. In certain locations, the peak width (FWHM) increases, suggesting the presence of distributed MgO particles at the nanoscale. The MgO doping caused crystalline phases to develop, whereas the pure blend has an amorphous shape. At 30 % MgO, the rise in crystallinity is especially noticeable [47].

SEM images of the pure blend and 10 %, 20 %, 30 % MgO added blend composite are given in Figure 4. The SEM image of the Pure Blend sample shows that the polymers of the Blend are very well bonded and form ring-shaped structures, while in the composite obtained with 30 % MgO addition, it was observed that the ring-shaped structures grew and nanoparticles formed at their boundaries [48]. This formation can be called a surface roughness and morphological irregularity [49]. The addition of MgO to the PVC–PCL blend alters the surface morphology. This enables strength and barrier gains in polymer nanocomposites with well-dispersed low-to-medium filler contents due to interfacial interactions. However, as the filler content increases, agglomeration becomes more pronounced and limits performance [50–52]. Indeed, in polymer systems containing MgO, it has been reported that at filler levels around 10 wt%, there is a more homogeneous distribution

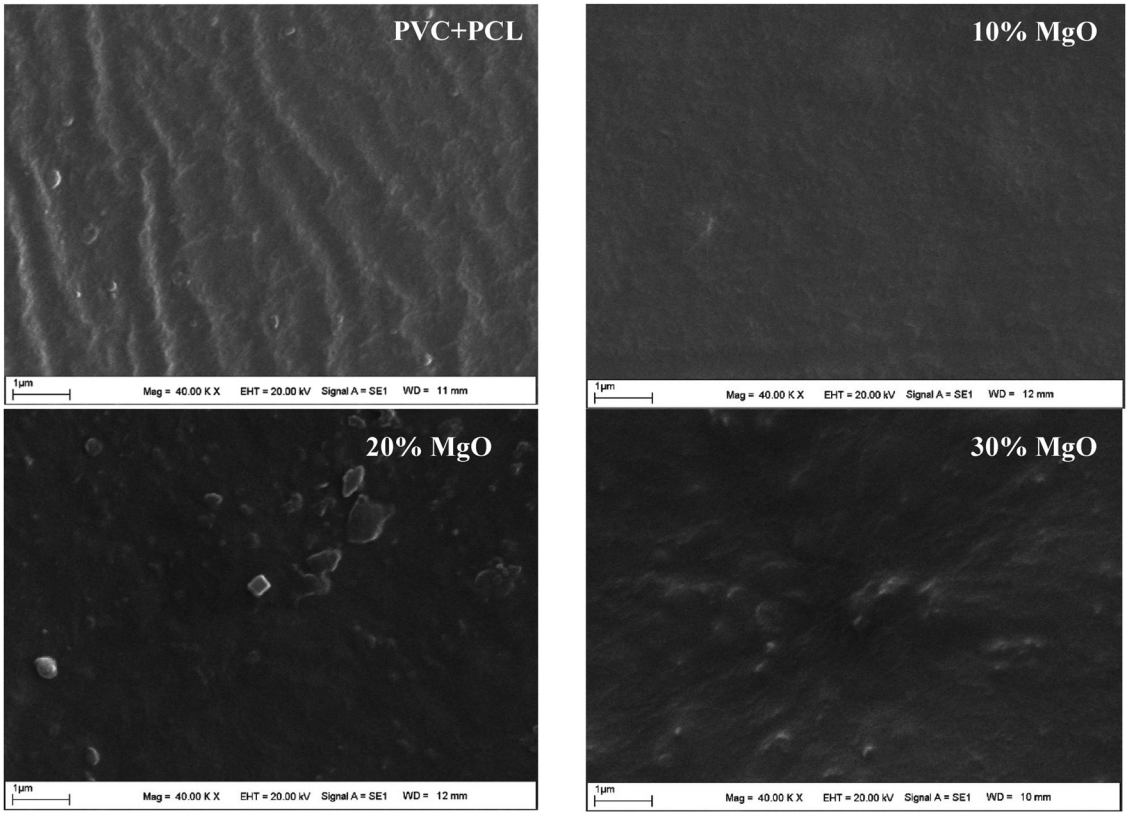

Figure 4: SEM image of blend and 10 %, 20 %, 30 %MgO blend composites.

and better mechanical response. Furthermore, agglomerates and associated reductions in tensile strength/toughness are frequently observed at levels of at least 15 wt% in SEM [50]. Similarly, it is emphasized that in PVC-based systems, oxide nanofillers (e.g., ZnO) intermix above a certain threshold due to their high surface energy, which has a negative effect on morphology and properties [53]. The presence of MgO can be observed in FTIR by Mg–O vibration bands in the 400–600 cm^{-1} range. The overlap of these bands with modes in the low wave number region of the polymer can cause overlapping, especially at high filler contents [54, 55] As a result, it can be said that the 10–20 % range offers better distribution and performance balance, but the 30 % range may cause increased agglomeration surface roughness and micro-defects.

DSC (differential scanning calorimetry) analysis (Figure 5) shows that the sample is a polymer blend containing polycaprolactone (PCL) and polyvinyl chloride (PVC). PCL is a semi-crystalline polymer and typically has a melting temperature (T_m) of 55–65 °C [56, 57]. The glass transition temperature (T_g) of amorphous PVC is approximately 75–85 °C [45, 58, 59]. The characteristic thermal transitions of both components in DSC analysis indicate that these polymers show phase separation in the blend and are thermally independent of each other. The effect of MgO on this structure suggests that the miscibility of PCL and PVC in this case is limited. MgO acts as a nucleating agent and changes the crystallization behavior in the polymer matrix. The increase in enthalpy change in DSC results shows that MgO increases the degree of crystallization of the mixture. It also produces a change towards a decrease in the melting peak. MgO may cause this increase by contributing to a more ordered crystallization of PCL chains [59]. The dispersion behavior of MgO in the PVC matrix and polymer-filler interfacial interactions may slightly change the thermal transition temperatures. This additive can not only increase the thermal stability, but also change the morphological properties of the structure, which makes it possible to obtain a thermoplastic material more suitable for use [60].

Thermogravimetric analysis (TGA) is a widely used thermal analysis method to learn the thermal stability and degradation behavior of polymeric materials. The obtained findings show that there is a significant difference between the degradation mechanisms between MgO nanoparticle doped composites and PCL–PVC blends (Figure 6). The mass loss in the MgO-containing composites was in four steps, while the PCL-PVC blend was in three steps. Evaporation of water trapped in the structure or physically adsorbed on the surface during the synthesis of MgO nanoparticles may cause this additional degradation step [59]. Due to the hygroscopic character of MgO, the water adsorption capacity increases with increasing surface area, especially

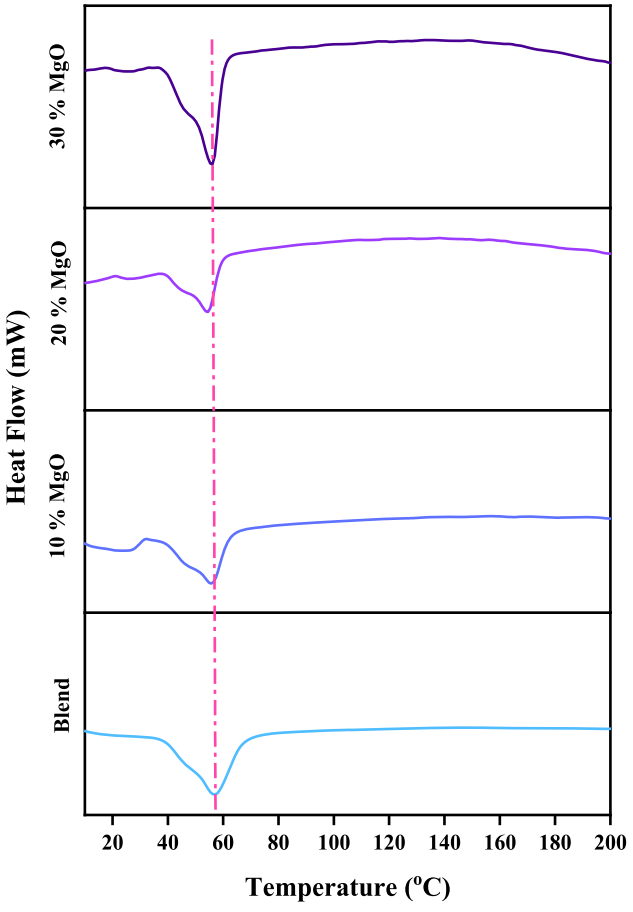

Figure 5: Heat flow curves of blend and composites.

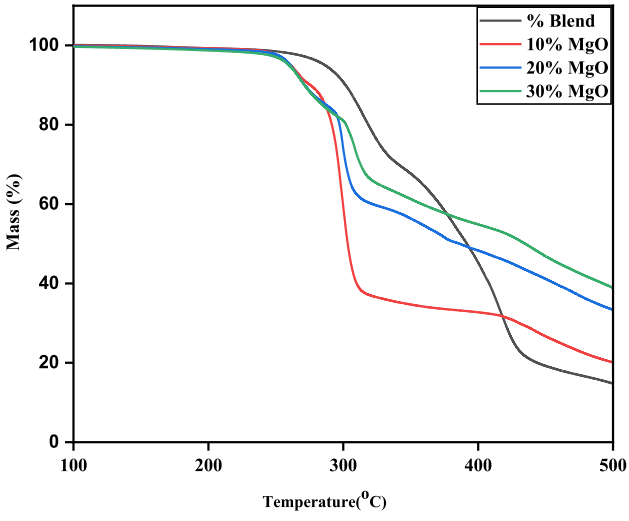

Figure 6: Thermogravimetric curve of blend and composites.

Table 2: Remain mass values of blend and composites.

Composite	Remain mass (%)
Blend	14.9
10 %	20.0
20 %	33.7
30 %	38.9

at the nanoparticle size [61]. The evaporation of this water usually takes place between 100 and 200 °C, supporting the fact that the first degradation step starts at earlier temperatures. MgO nanoparticle doping caused an earlier onset of thermal degradation compared to the blend. This provides evidence that hydroxyl groups on the MgO surface or acidic or basic surface properties can accelerate the degradation of polymer chains. Such interactions are referred to in the literature as "heterogeneous catalytic degradation" and are often mentioned with some inorganic additives [59]. In this case, MgO is both a physical filler material and an active component that can influence thermal degradation. Table 2 gave remain mass rate of blend and it MgO composites. These results can be explained by the fact that MgO has high thermal stability and does not degrade, leaving more inorganic residues in the structure at the end of degradation. This increase also indicates an increase in the inorganic/organic ratio of MgO, which is directly related to the amount of doping.

In PCL-PVC blend, the absorbance of the composites in the UV region generally increases as the MgO additive content increases (Figure 7). This is due to the fact that MgO

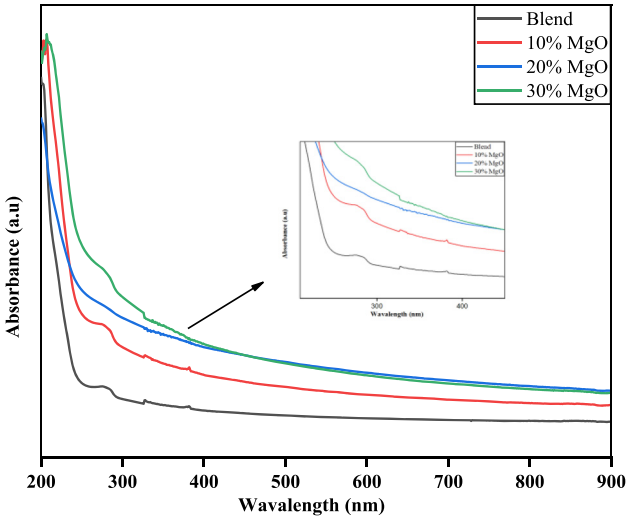

Figure 7: Wavelength dependent ultraviolet-visible absorption spectra for nanocomposites.

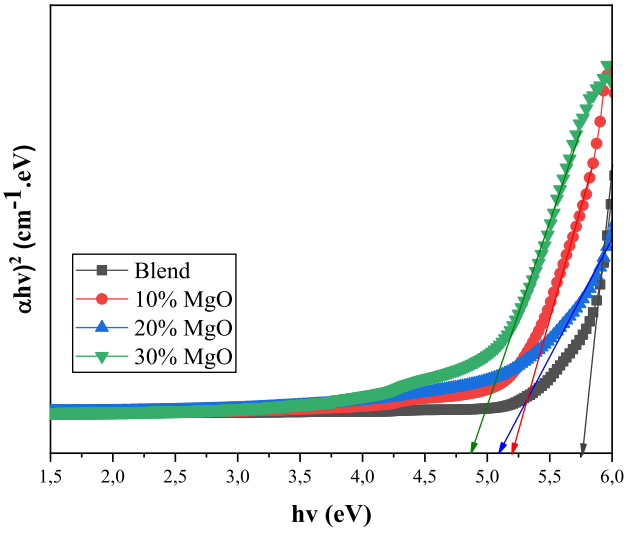

Figure 8: Tauc plots for nanocomposites.

nanoparticles have a high surface area and facilitate photon absorption. The gradual increase in absorbance values between 10 %, 20 % and 30 % MgO doping ratios indicates that the additive directly affects the ability to interact with light. Figure 8 shows the Tauc plots. The graph below shows the relationship between the optical absorption coefficient α and the bandgap E_g in the direct transition [48, 62, 63].

$$\alpha h\nu = A\left(h\nu - E_g\right)^{1/2}$$

The Tauc parameter, denoted as 'A', is a constant that quantifies the disorder within a crystal structure. It is influenced by the probability of electrical transitions and the distribution of band state densities at the tails. The Tauc plot is a graphical representation of the relationship between the square of the absorption coefficient $(\alpha h\nu)^2$ and photon energy ($h\nu$). Furthermore, the bandgap energy (E_g) of a material can be determined by extrapolating the linear region of the Tauc plot to the x-axis. A change in the slope of the extrapolation line indicates a corresponding change in the bandgap energy (E_g) [48, 62, 63]. The findings in the Table 3 show that the band gap (E_g) decreases when MgO is added to the PCL-PVC polymer matrix. These findings reveal that MgO changes the optoelectronic properties of PCL-PVC matrix. The band gap decreases as the MgO doping increases. Local energy levels and defect levels formed by the integration of MgO nanoparticles into the polymer matrix may explain this phenomenon. These levels create new energy levels between the fundamental band and the conduction band. These levels allow electrons to be excited using less energy. Therefore, the optical band gap becomes smaller. Other MgO-doped polymer systems have similar effects. For example, Shruthi K. N et al. showed that MgO

Table 3: Band gap energy values and opacity of blend and its MgO nanocomposites.

Samples	E_g (eV)	Opacity (mm^{-1})
PCL–PVC blend	5.77	2.82
10 % MgO	5.20	8.52
20 % MgO	5.11	13.72
30 % MgO	4.88	13.15

nanoparticles reduce the band gap in the PMMA matrix and are related to the energy levels that arise due to the interaction of MgO with the matrix [64, 65]. In addition, many literature studies have shown that nanoparticle doped interfaces increase polarizability by changing the optical properties. As a result, photon absorption shifts to lower energies and E_g value decreases [66, 67]. This band gap decrease in polymer nanoparticle composites is critical for improving light absorption properties, especially in ultraviolet (UV) protective applications or optoelectronic devices [68, 69]. The decrease in the band gap with increasing MgO doping ratio indicates that this composite material can be used as a better barrier against ultraviolet radiation. It can also be used in optoelectronic applications operating in the low energy range.

Opacity is the second most frequently employed criterion to assess the transparency of a film. A high opacity value signifies low sample transparency. The ratio of absorbance at 600 nm to the sample thickness in millimeters which measured by using ellipsometer is a form of normalization referred to as opacity. In this context, “absorbance” is understood to represent the logarithm of the inverse of transmittance, without implying whether the attenuation of the incident beam is due to absorption or reflection [70]. A UV-visible spectrophotometer was used to test the light transmittance of the film composites in order to determine their opacity. The following formula was used to determine the opacity values [71].

$$\text{Opacity} = \frac{A_{600}}{L}$$

In this equation, A_{600} is the absorbance at 600 nm and L is the film thickness (mm) [71]. Higher opacity values indicate lower film transparency. In the PCL-PVC blend and composite systems examined in the study, opacity values increased as the MgO NPs additive ratio increased (Table 3). The opacity value increased from 8.52 to 13.72 with the increase of MgO additive from 10 % to 20 %. The high refractive index of MgO may reduce the light transmittance of the material. However, after 30 % MgO doping, the opacity value dropped to 13.15, indicating a break in the upward trend. Despite this increase in MgO content, the decrease in the opacity value suggests that the use of high-content additives may cause particle agglomeration. Agglomeration reduces the scattering effect of light and disrupts the homogeneous distribution [72]. As a result, it can be concluded that 20 % of MgO doping is an ideal opacity ratio for this system. These results suggest that additive ratios should be carefully optimized to control the optical properties of composites.

Figure 9 experimentally demonstrates the shape memory behavior of MgO-modified PCL-PVC thin film composites. A classical shape memory cycle was applied to investigate the shape memory properties of the prepared samples. In the first stage, the samples were heated to approximately 55 °C (close to the melting temperature of PCL) and held at this temperature for 5 min. This process allows the crystalline regions of PCL to partially melt and increases the mobility of the polymer chains. This allowed a temporary shape (e.g., bending or curling) to be manually imparted to the material. In the second stage, the samples were rapidly transferred to an ice bath for sudden cooling. This cooling promoted the recrystallization of the PCL chains, locking in the temporary shape. Thus, the crystalline regions formed within the polymer matrix restricted chain movements and stabilized the temporary form of the sample. In the third stage, the samples fixed in their temporary shape were reheated to approximately 55 °C. At this temperature, the crystalline regions of PCL melt again and chain mobility increases. As a result, the material releases the applied temporary shape and returns to its original form. Experimental observations show that MgO reinforcement plays an important role in this cycle. MgO nanoparticles contribute to the more stable fixation of the temporary shape by affecting the crystallization behavior within the polymer matrix and, at the same time, increase the shape recovery rate by facilitating chain mobility during heating. Therefore, it can be concluded that MgO-reinforced PCL-PVC thin film composites exhibit high shape memory performance, with quite successful temporary shape fixation ratios and shape recovery ratios.

In addition to the structural and optical characterizations, the prepared films’ weight and cost were also considered from a practical perspective. Because of the increasing inorganic fraction in the structure, the overall mass of each composite increased somewhat as the MgO content increased. However, even at larger loadings, the total material cost remained economically viable due to the cheap cost, chemical stability, and commercial availability of MgO nanoparticles [23, 24, 26]. Given the comparatively low additive ratios (10–30 wt percent), the significant increases in thermal stability and UV-shielding effectiveness outweigh the cost increase per sample. For industrial and

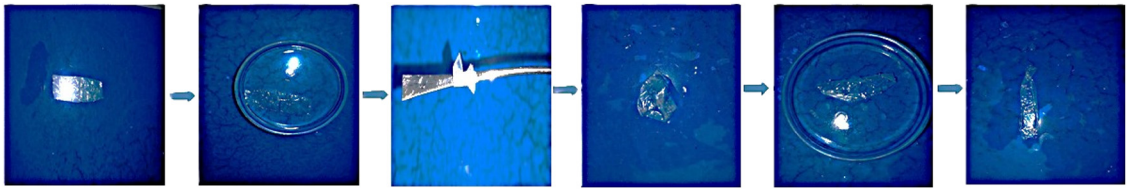

Figure 9: Shape memory effect of the polymer composite thin film added to the PCL-PVC polymer blend with 20 % MgO.

packaging applications, MgO-reinforced PCL–PVC nanocomposite films can thus be considered a scalable and reasonably priced material [28, 29].

4 Conclusions

The developed MgO-reinforced PCL-PVC nanocomposite films demonstrate strong potential for UV protected packaging and optoelectronic applications due to simultaneous gains in structural integrity, thermal stability, and optical performance. FTIR characteristics, particularly in the carbonyl and ether regions, confirm robust filler-matrix interactions, while XRD confirms the presence of crystalline MgO and an increase in overall crystallinity depending on loading. SEM observations reveal composition-dependent morphology: good dispersion and interfacial adhesion at moderate MgO content, while surface roughness due to agglomeration becomes more pronounced at higher loadings. Thermally, MgO acts as an effective nucleation agent and shifts decomposition to higher inorganic residues, supporting improved high-temperature stability. Optically, MgO increases UV absorbance and lowers the Tauc band gap (E_g), consistent with enhanced photon absorption; opacity in the visible range peaks at 20 % by weight, followed by a slight decrease to 30 % by weight, which is likely due to nanoparticle agglomeration. When these results are combined, 20 % MgO by weight is positioned as a balanced formulation for homogeneous opacity and processability, while higher loadings can be utilized when maximum UV attenuation and E_g reduction are prioritized, provided that dispersion is carefully controlled.

Acknowledgments: The authors would like to thank the financial support provided by the Management Unit of the Scientific Research Projects of Firat University (FUBAP) (Project Number: FF 25.21 and ADEP 25.05).
Funding information: This work was funded by Management Unit of the Scientific Research Projects of Firat University (FUBAP) (Project Number: FF 25.21 and ADEP 25.05).

Author contributions: Meltem Coşkun – methodology and writing-review and editing; Ecem Özen Öner –writing-original draft; Cengiz Tatar and Mediha Kök –writing, supervision, and project manage. All authors have accepted responsibility for the entire content of this manuscript and approved its submission.
Conflict of interest: The authors state no conflict of interest.
Data availability statement: All data generated or analyzed during this study are included in this published article.

References

1. Gigante V, Aliotta L, Ascrizzi R, Pistelli L, Zinnai A, Batoni G, et al. Innovative biobased and sustainable polymer packaging solutions for extending bread shelf life: a review. Polymers 2023;15:4700.
2. Silvestre C, Duraccio D, Cimmino S. Food packaging based on polymer nanomaterials. Prog Polym Sci 2011;36:1766—82.
3. Huang H-D, Ren P-G, Zhong G-J, Olah A, Li Z-M, Baer E, et al. Promising strategies and new opportunities for high barrier polymer packaging films. Prog Polym Sci 2023;144:101722.
4. Dobiáš J, Voldřich M, Marek M, Chudáčková K. Changes of properties of polymer packaging films during high pressure treatment. J Food Eng 2004;61:545—9.
5. Alin J, Hakkarainen M. Type of polypropylene material significantly influences the migration of antioxidants from polymer packaging to food simulants during microwave heating. J Appl Polym Sci 2010;118:1084—93.
6. Malikmammadov E, Tanir TE, Kiziltay A, Hasirci V, Hasirci N. PCL and PCL-based materials in biomedical applications. J Biomater Sci Polymer edition. 2018;29:863—93. .
7. Mohamed RM, Yusoh K. A review on the recent research of polycaprolactone (PCL). Adv Mater Res 2016;1134:249—55.
8. Dash TK, Konkimalla VB. Polymeric modification and its implication in drug delivery: Poly-ε-Caprolactone (PCL) as a model polymer. Mol Pharm 2012;9:2365—79.
9. Woodruff MA, Hutmacher DW. The return of a forgotten polymer—Polycaprolactone in the 21st century. Prog Polym Sci 2010;35:1217—56.
10. Rezgui F, Swistek M, Hiver J, G'sell C, Sadoun T. Deformation and damage upon stretching of degradable polymers (PLA and PCL). Polymer 2005;46:7370—85.
11. Leadbitter J. PVC and sustainability. Prog Polym Sci 2002;27:2197—226.

12. Daniels PH. A brief overview of theories of PVC plasticization and methods used to evaluate PVC-plasticizer interaction. J Vinyl Addit Technol 2009;15:219—23.
13. Yu J, Sun L, Ma C, Qiao Y, Yao H. Thermal degradation of PVC: a review. Waste Manag 2016;48:300—14.
14. Li W, Bai Z, Zhang T, Jia Y, Hou Y, Chen J, et al. Comparative study on pyrolysis behaviors and chlorine release of pure PVC polymer and commercial PVC plastics. Fuel 2023;340:127555.
15. Coleman M, Zarian J. Fourier-transform infrared studies of polymer blends. II. Poly (ϵ-caprolactone)-poly (vinyl chloride) system. J Polym Sci Polym Phys Ed 1979;17:837—50.
16. Mamun A, Mareau VH, Chen J, Prud'homme RE. Morphologies of miscible PCL/PVC blends confined in ultrathin films. Polymer 2014;55:2179—87.
17. Mohammed AA, Habeeb MA. Effect of Si3N4/TaC nanomaterials on the structural and electrical characteristics of poly methyl methacrylate for electrical and electronics applications. East Eur J Phys 2023:157—64. https://doi.org/10.26565/2312-4334-2023-2-15.
18. Hamza RSA, Habeeb MA. Reinforcement of morphological, structural, optical, and antibacterial characteristics of PVA/CMC bioblend filled with SiO2/Cr2O3 hybrid nanoparticles for optical nanodevices and food packing industries. Polym Bull 2024;81:4427—48.
19. Algidsawi AJK, Hashim A, Hadi A, Habeeb MA, Abed HH. Influence of MnO2 nanoparticles addition on structural, optical and dielectric characteristics of PVA/PVP for pressure sensors. Phys Chem Solid State 2022;23:353—60.
20. Oreibi I, Ali HM, Abdul Hamza RS. Polymer nanocomposites comprising PVA matrix and Ag—BaTiO3 nanofillers: a comparative study of structural, dielectric and optical characteristics for optics and quantum nanoelectronic applications. Opt Quant Electron 2024;56:119.
21. Muzata TS, Gebrekrstos A, Orasugh JT, Ray SS. An overview of recent advances in polymer composites with improved UV-shielding properties. J Appl Polym Sci 2023;140:e53693.
22. Mohammadi M, Asadi Mamdooh H, Shirkavand Hadavand B. Synthesis and characterization of UV curable polyurethane-acrylate nanocomposite-based coatings enhanced with magnesium fluoride nanoparticles. J Macromol Sci, Part A 2024;61:760—71.
23. Chinthala M, Balakrishnan A, Venkataraman P, Manaswini Gowtham V, Polagani RK. Synthesis and applications of nano-MgO and composites for medicine, energy, and environmental remediation: a review. Environ Chem Lett 2021;19:4415—54.
24. Baysal T, Noor N, Demir A. Nanofibrous MgO composites: structures, properties, and applications. Polym Plast Technol Mater 2020;59:1522—51.
25. Aničić N, Kurtjak M, Jeverica S, Suvorov D, Vukomanović M. Antimicrobial polymeric composites with embedded nanotextured magnesium oxide. Polymers 2021;13:2183.
26. Cha H-A, Ha S-J, Jo M-G, Moon YK, Choi J-J, Hahn B-D, et al. Three-dimensional MgO filler networking composites with significantly enhanced thermal conductivity. Adv Compos Hybrid Mater 2024;7:178.
27. Hajibeygi M, Mousavi M, Shabanian M, Habibnejad N, Vahabi H. Design and preparation of new polypropylene/magnesium oxide micro particles composites reinforced with hydroxyapatite nanoparticles: a study of thermal stability, flame retardancy and mechanical properties. Mater Chem Phys 2021;258:123917.
28. Swaroop C, Shukla M. Nano-magnesium oxide reinforced polylactic acid biofilms for food packaging applications. Int J Biol Macromol 2018;113:729—36.
29. Oluwafunke O, Okonkwo TP, Amienghemhen OD, Oyegoke J, Ifeanyi OA, Ifijen IH, et al. Applications of polylactic acid-magnesium composite materials for sustainable packaging solutions. In: Al Majari Y, Wisner B, Mastorakos IN, Murph SEH, Paramsothy M, editors. Advances in sustainable composites. Cham: Springer; 2025:163—81 pp.
30. Islam MS, Elahee GF, Fang Y, Yu XB, Advincula RC, Cao CC. Polylactic acid (PLA)-Based multifunctional and biodegradable nanocomposites and their applications. Compos B Eng 2025;306:112842.
31. García-Sobrino R, Muñoz M, Rodríguez-Jara E, Rams J, Torres B, Cifuentes SC. Bioabsorbable composites based on polymeric matrix (PLA and PCL) reinforced with magnesium (mg) for use in bone regeneration therapy: physicochemical properties and biological evaluation. Polymers 2023;15:4667.
32. Tripathi V. Hydrothermal method for synthesis of materials. In: Handbook on synthesis strategies for advanced materials. Singapore: Springer; 2021:131—52 pp.
33. Jayatissa YXGAH, Yu Z, Chen X, Li M. Hydrothermal synthesis of nanomaterials. J Nanomater 2020;2019. NA-NA.
34. Schäf O, Ghobarkar H, Knauth P. Hydrothermal synthesis of nanomaterials. In: Nanostructured materials: selected synthesis methods properties and applications. New York: Springer; 2004: 23—41 pp.
35. Phillipson K, Jenkins MJ, Hay JN. The kinetics of crystallization of poly (ε-caprolactone) measured by FTIR spectroscopy. J Therm Anal Calorim 2016;123:1491—500.
36. Phillipson K, Hay J, Jenkins M. Thermal analysis FTIR spectroscopy of poly (ε-caprolactone). Thermochim Acta 2014;595:74—82.
37. Rahmatabadi D, Yousefi MA, Shamsolhodaei S, Baniassadi M, Abrinia K, Bodaghi M, et al. 4D printing of polyethylene glycol-grafted carbon nanotube-reinforced polyvinyl chloride—polycaprolactone composites for enhanced shape recovery and thermomechanical performance. Adv Intell Syst 2025;7:2500113.
38. Balakrishnan G, Velavan R, Batoo KM, Raslan EH. Microstructure, optical and photocatalytic properties of MgO nanoparticles. Results Phys 2020;16:103013.
39. Salman KD, Abbas HH, Aljawad HA, editors. Synthesis and characterization of MgO nanoparticle via microwave and sol-gel methods. Journal of Physics: Conference Series. Bristol: IOP Publishing; 2021.
40. Keledi G, Hári J, Pukánszky B. Polymer nanocomposites: structure, interaction, and functionality. Nanoscale 2012;4:1919—38.
41. Baji A, Mai Y-W, Wong S-C, Abtahi M, Chen P. Electrospinning of polymer nanofibers: effects on oriented morphology, structures and tensile properties. Compos Sci Technol 2010;70:703—18.
42. Kun Z, Fang H, Huang Z, Wei G-q, Zheng A-q, Li H-b, et al. CaO/MgO modified perovskite type oxides for chemical-looping steam reforming of methane. J Fuel Chem Technol 2016;44:680—8.
43. Kim P, Lee CJ. The reduction temperature effect of Fe—co/MgO catalyst on characteristics of multi-walled carbon nanotubes. Catalysts 2018;8:361.
44. Liu W, Zhang R, Huang M, Dong X, Xu W, Ray N, et al. Design and structural study of a triple-shape memory PCL/PVC blend. Polymer 2016;104:115—22.

45. Pekdemir ME, Öner E, Kök M, Qader IN. Thermal behavior and shape memory properties of PCL blends film with PVC and PMMA polymers. Iran Polym J (Engl Ed) 2021;30:633–41.
46. Martins-Franchetti SM, Egerton T, White J. Morphological changes in poly (caprolactone)/poly (vinyl chloride) blends caused by biodegradation. J Polym Environ 2010;18:79–83.
47. Venugopal G, George R, Raghavan N, Srinivas T, Dakshinamurthy A, Paul AJ, et al. Structural and mechanical properties of MgO-poly (vinyl alcohol) nanocomposite film. Adv Sci Eng Med 2015;7:457–64.
48. Özen Öner E, Tatar C, Kök M. Synthesis, characterization, optical and gamma shielding properties of La2O3 doped recycled PS-PVC/PCL ternary blend composites. J Polym Environ 2025;33:2920–30.
49. Qader IN, Kök M, Mohammed KS, Coskun M, Öner EÖ, Aydoğdu Y. Development of a PLA/PHA-TiO_2 polymer blend with improved physicochemical and thermal properties. J Polym Environ 2025:1–13.
50. Hachani SE, Meghezzi A, Nebbache N, Slimani M. Impact of magnesium oxide incorporation on tensile and hardness properties of polystyrene/magnesium oxide composites. J Chem Pharmaceut Sci 2016;9:2664–7.
51. Santagiuliana G, Picot OT, Crespo M, Porwal H, Zhang H, Li Y, et al. Breaking the nanoparticle loading–dispersion dichotomy in polymer nanocomposites with the art of croissant-making. ACS Nano 2018;12:9040–50.
52. Fu S, Sun Z, Huang P, Li Y, Hu N. Some basic aspects of polymer nanocomposites: a critical review. Nano Mater Sci 2019; 1:2–30.
53. Faiza KA, Alahmadi AA, Ishida H, Ullah N. Improved PVC/znO nanocomposite insulation for high voltage and high temperature applications. Sci Rep 2023;13:7235.
54. Umaralikhan L, Jamal MJM. Green synthesis of MgO nanoparticles and it antibacterial activity. Iran J Sci Technol Trans A-Science 2018;42:477–85.
55. Radulescu D-M, Neacsu IA, Vasile BS, Surdu V-A, Oprea O-C, Trusca R-D, et al. Green-synthesized MgO nanoparticles: structural insights and antimicrobial applications. Int J Mol Sci 2025;26: 9021.
56. Aoyama T, Uto K, Shimizu H, Ebara M, Kitagawa T, Tachibana H, et al. Development of a new poly-ε-caprolactone with low melting point for creating a thermoset mask used in radiation therapy. Sci Rep 2021;11:20409.
57. Luna CBB, Siqueira DD, Ferreira ESB, Araujo EM, Wellen RMR. Effect of injection parameters on the thermal, mechanical and thermomechanical properties of polycaprolactone (PCL). J Elastomers Plast 2021;53:1045–62.
58. Sorolla-Rosario D, Llorca-Porcel J, Pérez-Martínez M, Lozano-Castelló D, Bueno-López A. Study of microplastics with semicrystalline and amorphous structure identification by TGA and DSC. J Environ Chem Eng 2022;10:106886.
59. Aberoumand M, Soltanmohammadi K, Rahmatabadi D, Soleyman E, Ghasemi I, Baniassadi M, et al. 4D printing of polyvinyl chloride (PVC): a detailed analysis of microstructure, programming, and shape memory performance. Macromol Mater Eng 2023;308:2200677.
60. Li Q, Shen F, Ji J, Zhang Y, Muhammad Y, Huang Z, et al. Fabrication of graphite/mgO-Reinforced poly (vinyl chloride) composites by mechanical activation with enhanced thermal properties. RSC Adv 2019;9:2116–24.
61. Proniewicz E, Vijayan AM, Surma O, Szkudlarek A, Molenda M. Plant-assisted green synthesis of MgO nanoparticles as a sustainable material for bone regeneration: spectroscopic properties. Int J Mol Sci 2024;25:4242.
62. Hong S. Investigation of gradient band gap in Cu2ZnSnS4 thin films with residual strain. Curr Appl Phys 2024;58:65–73.
63. Tatar C, Kök M, Doğru M, Coşkun M, Özen Öner E. Detailed physical property investigation study on ZnO NPs containing waste PS-PLA smart polymeric composites: crystal structure, thermal, optical properties and radiation shielding behavior. Macromol Res 2025;33:1097–107.
64. Shruthi K, Varma VR, Kumar M, Sanjeev G, editors. Structural and Optical Properties of PMMA-MgO Nanocomposite Film. IOP Conference Series: Materials Science and Engineering. Bristol: IOP Publishing; 2024.
65. Bdewi SF, Abdullah OG, Aziz BK, Mutar AA. Synthesis, structural and optical characterization of MgO nanocrystalline embedded in PVA matrix. J Inorg Organomet Polym Mater 2016;26:326–34.
66. Sayed AME, Abdelghany A, Abou Elfadl A. Structural, optical, mechanical and antibacterial properties of MgO/poly (vinyl acetate)/poly (vinyl chloride) nanocomposites. Braz J Phys 2022;52:150.
67. Salim E, Abdelghany A, Tarabiah A. Ameliorating and tuning the optical, dielectric, and electrical properties of hybrid conducting polymers/metal oxide nanocomposite for optoelectronic applications. Mater Chem Phys 2024;313:128788.
68. Agrahari S, Singh SP, Gupta AK. Effect of MgO NPs doping on the optoelectronic and electrochemical behavior of polyethylene oxide (PEO) nanocomposite polymer electrolyte. J Phys Chem Solid 2025;203:112706.
69. Shamekh A, Shaalan N, Hanafy T, Rashad M. Linear/Nonlinear optical properties of functional inorganic MgO nano-filler in PVA transparent polymer for flexible optoelectronic devices. Phys B Condens Matter 2023;651:414617.
70. Guzman-Puyol S, Benítez JJ, Heredia-Guerrero JA. Transparency of polymeric food packaging materials. Food Res Int 2022;161:111792.
71. Aydogdu A, Radke CJ, Bezci S, Kirtil E. Characterization of curcumin incorporated guar gum/orange oil antimicrobial emulsion films. Int J Biol Macromol 2020;148:110–20.
72. Lizundia E, Vilas JL, Sangroniz A, Etxeberria A. Light and gas barrier properties of PLLA/Metallic nanoparticles composite films. Eur Polym J 2017;91:10–20.